Electronic Supplementary Material (ESI) for Sustainable Energy & Fuels.

A techno-economic analysis method for guiding research and investment directions for c-Si Photovoltaics and its application to Al-BSF, PERC, LDSE and Advanced Hydrogenation

Nathan L. Chang, Anita Ho-Baillie, Stuart Wenham, Michael Woodhouse, Rhett Evans, Budi Tjahjono, Fred Qi, Chee Mun Chong and Renate J. Egan

Supplementary Material

S1 Process and Factory Assumptions

S1.1 Sequence Definitions

Some details of the sequences analysed in this work are given in Table S1, and the process steps assumed for each sequence are shown in Table S2.

Table S1 Demonstrated results using these different sequences

Sequence	A: Al-BSF	B: PERC	C: LDSE	D: PERC+LDSE	E:PERC+LaserH	F:PERC+LEDH	G:PERC+FurnH
Status	Industrial production [1]	Industrial production [1]	Previous industrial production [2]	Lab Demo[3, 4]	Lab demo [5]	Lab Demo[6]	Described [5]

Table S2 Definitions of Process Sequences A (Al BSF), B (PERC), C (LDSE), D (LDSE + PERC), E (PERC + LaserH), F (PERC + LEDH) and G (PERC + FurnH)

A	B	C	D	E	F	G	Process Description	Equipment	Major materials
X	X	X	X	X	X	X	p-type Wafer supply	None	p-type Wafer
X	X	X	X	X	X	X	Texture	Texture Tool	Texture Chemicals
X	X	X	X	X	X	X	Diffusion	Diffusion Furnace	Diffusion Gases
X	X	X	X	X	X	X	Rear etch	Etch Tool	Etch chemicals
		X	X				Oxide Layer	Oxidation Furnace	Process Gases
X	X	X	X	X	X	X	Front SiN	PECVD	SiN Gases
	X		X	X	X	X	Rear Passivation Layers	PECVD	SiN/AlOx Gases
	X		X	X	X	X	Dielectric Openings	Laser	None
X	X	X	X	X	X	X	Rear Screen print Ag/Al	Screen Printer	Ag and Al paste
X	X			X	X	X	Front Screen Print Ag	Screen Printer	Ag paste
X	X	X	X	X	X	X	Standard Firing	Firing Furnace	
						X	Hydrogenation add-on	Firing Furnace Upgrade	
		X	X				Dopant Application	Spray coater	Phosphoric acid
		X	X				Laser Doping	Laser	None
		X	X				Ni/Cu/Ag Plating	Plating Equipment	Plating solutions
		X	X				Nickel Sinter process		
				X			Laser Hydrogenation	Hydrogenation Laser	
					X		LED Hydrogenation	Hydrogenation LED System	
X	X	X	X	X	X	X	Cell test	Cell tester and sorter	None
X	X	X	X	X	X	X	Module fabrication	Module Line	Module Materials

S1.2 Other Factory Assumptions

Various factory global assumptions are shown in Table S3. Note that unlike other parameters in this analysis, these assumptions do not vary within the Monte Carlo analysis.

S2 Data Sources and Assumptions

S2.1 Cell Fabrication Cost Data Sources

Detailed costs of the standard production processes (e.g. equipment cost, volume material purchase prices, manufacturing yield) are not generally made public by manufacturing companies. Manufacturing companies see cost information as a source of competitive advantage, and negotiated pricing is often “commercial in confidence”. In some cases an industry-institute collaboration exists, and this

Table S3 Factory Assumptions

Parameter	Assumption	Comment
Factory location	China	Most PV manufacturing is in China
Factory start date	2017	
Factory Throughput (modules/year)	1.6 Million	Matching the size of Powell et al. model
Factory Throughput (MW/year at 280W/module)	450	
Depreciation time - Equip and Facilities	7 years	
Depreciation time - Building	15 years	
Currency for Calculations	US$	
Operator Cost ($/h)	8.3	Goodrich et al. [7] + estimated wage inflation
Maintenance Technician Cost ($/h)	12.1	Goodrich et al. [7] + estimated wage inflation
Indirect Labour cost ratio	0.1	Estimate based on Powell's c-Si cost model [8]
Floor space ratio (total/footprint)	3	
Building cost per m^2	1000	Estimate
Building and Facility maintenance rate	4% of capex per year	Estimate
Electricity Cost	US$0.08 / kWh	Goodrich et al. [7] advanced scenario
Electricity for Services	1 kWh / tool kWh	Exhaust, cooling water, Air con

information may be shared with the institute. However confidentiality agreements usually mean that such data and the resulting analysis cannot be published. In this fast changing industry, economies of scale and incremental improvements to processes and performance can quickly change the cost analysis results so that such cost analysis work can quickly become outdated. Commercial R&D teams have an advantage in this area, being linked to manufacturing companies, as cost data is usually available for them to make more informed analysis and decisions.

For production processes that vary from the industry standard, the toolset costs (particularly at high volume production) may not be known. It may be possible to obtain the price of a single lab or pilot production tool, but this would not reflect the real cost of production when scaled up. Again, institutes are at a disadvantage here, in that equipment vendors are unlikely to provide accurate cost data without the prospect of a tool sale.

The cost of the incoming wafer is approximately half of the total cost of producing a cell. In this model, we have not modelled the cost of producing polysilicon, and transforming this into an ingot and then wafering. Instead we have taken 6 months of historical average mono wafer price data from Energytrend [9] from April, 2017 to Sept, 2017. We have used the average, low and high values as the parameter range for this material cost, as shown in Table 2.

The Al-BSF sequence is the current industry standard process. There exists some independent analyses of manufacturing cost for this sequence that are by nature less accurate that the "real" data from manufacturers, such as Powell et al. [10]. However this work was published in 2015, and has cost estimates far higher than the current prices in the market.

The PERC process has been analysed by Woodhouse et al. [11] (paper in preparation). They communicated with manufacturers to estimate the cost of setting up state of the art manufacturing lines in wafer, cell (PERC) and module manufacture. With this data, they calculated the cost of production, and cross checked with commonly quoted metrics such as staff levels and electricity usage per unit of production. We have taken the summary cost data breakdown from that study as at May, 2017, which assumed 21.5 % cell efficiency, and translated this to parameters suitable for input into the cost model.

In order to generate the parameters used in our model, we had to make a number of assumptions, outlined here. The Woodhouse et al. summary cost data had a single value for depreciation that included the tool itself (7 year depreciation time) and facility/building (20 year depreciation time). We matched this depreciation value by modelling a value for tool cost, and a value for installation cost (being 15% of the tool cost), and zero floor space (and cost) for the building. The Woodhouse et

al. cost data showed average costs per process (in $/W), so to estimate the cost of each process tool we assumed a nominal 3200 wafer/h tool capacity. We also translated all costs into area related costs (i.e. $/cell or $/module) in order to separately analyse the impact of cell and module performance on cost.

With regard to uncertainty, as the Woodhouse et al. data is based on discussions with suppliers and manufacturers and not firm quotes for multiple tools as would be required to set up a factory, we have used uncertainty bounds of $\pm 30\,\%$ per tool cost, electricity usage and material costs and $\pm 5\,\%$ for the tool installation cost.

The Woodhouse et al. data was for a PERC sequence, so to estimate the Al-BSF sequence costs we extrapolated that the tool to deposit a single side front SiN layer would be 70% of the cost and would use 50% the materials of the double sided SiN tool. We also estimate that removing the front screen print step would reduce the cost of the printer/drier by 20% and save 50% of the paste costs.

The LDSE process is based on UNSW experience, and is similar to what was developed and implemented by Suntech in collaboration with UNSW in the "Pluto" Technology. UNSW has some cost estimates for the LDSE sequence that were developed in collaboration with industry partners, with some results of that analysis published by Edwards [12]. From this analysis we have extracted the cost of the LDSE specific steps (formation of an oxide layer, laser doping and plating) for use in our model. The most recent 2014 data from the UNSW model has been revised for changes in the capital cost, reflected elsewhere in the PV industry over the past 5 years, and to account for expected economies of scale from pilot production (80MW) to full scale manufacturing (>400MW). Specifically we have assumed that capital costs are 70% (uncertainty range 50% to 90%) of the 2014 value. For material costs, we have been very conservative, assuming that the costs are unchanged, but with an uncertainty range of $\pm$50%. Whilst further work could be done to refine these cost estimates, this has not been done in this study, and even with these large uncertainty bounds, we have determined that refining these costs is not critical to the analysis. The 2014 UNSW cost analysis did not include the improved anchor points process which we have assumed in this work. So we have assumed a 20% cost premium on the laser system cost to model the requirement for two laser processes within the same tool.

The Advanced Hydrogenation processes are based on discussions with equipment suppliers via the University of New South Wales Solar Industrial Research Facility (SIRF), where indicative single unit pricing was obtained [13]. We have taken these estimates, and projected an uncertainty range for purchasing multiple tools for a production line of 500MW.

The detailed parameters including the uncertainty ranges that were used in this study can be found in Tables S4, S5 and S6.

S2.2 Cell Performance

The various improved sequences defined in Table S2 generally increase the cost of production of each cell or module (the per unit area cost). This additional cost must be offset by an improvement in efficiency in order for a technology to have a lower cost per unit power ($/W) and higher selling price for the technology to make commercial sense.

Whilst some of these sequences have been successfully implemented in high volume production, and the performance improvement can be assessed, some sequences have only been tested in a lab or pilot production. We have estimated the expected cell efficiency performance as shown in Table 1. Because of the uncertainty in the actual performance gain should each sequence be established in commercial production, a Low and High range of efficiency gain is estimated and used in the Monte Carlo uncertainty analysis.

Table S4 Equipment Cost Input Assumptions and Uncertainty Ranges - Cost. These are all assumptions for a single production tool. The Tool Cost includes purchase and installation, facility cost includes purchase and installation of support services such as electricity, compressed air, electricity and chemical delivery. Floor space is the actual footprint of the equipment, which is used to calculate the size and cost of the building

Equipment	Tool Cost US$M	Facility Cost (% of Tool Cost)	Floor space m^2	Spare Parts (% Capex / year)	Electricity Usage (kW)	Reference
Wafer Inspection	0.671 (0.469-0.872)	15 (10-20)	0 (0-0)	8 (4-12)	33 (23-43)	[11]
Wafer Etch Bath	0.766 (0.536-0.996)	15 (10-20)	0 (0-0)	3 (2-4)	58 (40-75)	[11]
Diffusion Furnace	2.299 (1.609-2.989)	15 (10-20)	0 (0-0)	4 (2-6)	82 (58-107)	[11]
Rear etch bath	1.629 (1.14-2.117)	15 (10-20)	0 (0-0)	4 (2-6)	41 (29-53)	[11]
Oxidation Furnace	0.632 (0.541-0.722)	9 (5-14)	0 (0-0)	5 (3-7)	150 (100-200)	[12]
PECVD SiN - Single Side Processing	1.274 (0.892-1.656)	15 (10-20)	0 (0-0)	3 (2-4)	52 (36-67)	[11]
PECVD SiN - Upgrade to two sided processing	0.546 (0.382-0.71)	15 (10-20)	0 (0-0)	3 (2-4)	22 (16-29)	[11]
Rear AlOx passivation Tool	3.161 (2.213-4.11)	15 (10-20)	0 (0-0)	5 (2-8)	90 (63-118)	[11]
PERC Laser	1.437 (1.006-1.868)	15 (10-20)	0 (0-0)	2 (1-3)	74 (52-96)	[11]
Screen Printer (Additional front print	0.134 (0.094-0.174)	9 (5-14)	0 (0-0)	5 (3-7)	13 (9-17)	[11]
Screen Printer (2 prints)	0.536 (0.376-0.697)	15 (10-20)	0 (0-0)	2 (1-3)	53 (37-68)	[11]
Dopant Spray Coater	0.253 (0.217-0.289)	10 (5-15)	5 (4-7)	5 (3-10)	20 (15-25)	[12]
Doping Laser	0.583 (0.5-0.666)	5 (3-10)	10 (5-15)	10 (5-15)	5 (3-20)	[12]
Plating Tool	2.429 (2.082-2.776)	20 (10-30)	40 (30-60)	10 (5-15)	150 (100-200)	[12]
Sinter Furnace	0.359 (0.308-0.411)	10 (5-15)	20 (15-30)	5 (3-7)	15 (10-30)	[12]
Hydrogenation Laser	0.72 (0.64-0.8)	10 (5-15)	10 (8-11)	5 (3-7)	20 (15-25)	[13]
LED Hydrogenation	0.27 (0.24-0.3)	10 (5-15)	13 (11-15)	5 (3-7)	104 (93-116)	[13]
Hydrogenation Firing Furnace Upgrade	0.08 (0.055-0.103)	10 (5-16)	0 (0-0)	5 (3-7)	47 (33-61)	[13]
Firing Furnace	0.287 (0.201-0.374)	15 (10-20)	0 (0-0)	9 (4-14)	115 (81-150)	[11]
Cell test, sort and package	0.766 (0.536-0.996)	15 (10-20)	0 (0-0)	7 (4-10)	58 (40-75)	[11]

Table S5 Equipment Cost Input Assumptions and Uncertainty Ranges - Throughput and Staff. The throughput is the average during non-maintenance time. During normal tool operation, the specified number of operation staff are required to operate, load and monitor the equipment. During maintenance time, the specified number of maintenance staff are required to conduct preventative maintenance or repair

Equipment	Throughput	Units	Down Time (%)	# Staff (operation)	# staff (maintenance)	Reference
Wafer Inspection	3200 (3040-3360)	wafer/h	2 (1-5)	4 (3-5)	2 (1-3)	[11]
Wafer Etch Bath	3200 (3040-3360)	wafer/h	4 (2-6)	2 (1-3)	2 (1-3)	[11]
Diffusion Furnace	3200 (3040-3360)	wafer/h	3 (2-4)	1.5 (0.5-2.5)	2 (1-3)	[11]
Rear etch bath	3200 (3040-3360)	wafer/h	4 (2-6)	2 (1-3)	2 (1-3)	[11]
Oxidation Furnace	3000 (2400-3600)	wafer/h	3 (2-4)	0.5 (0.25-1)	2 (1-3)	[12]
PECVD SiN - Single Side Processing	3200 (3040-3360)	wafer/h	6 (4-8)	2 (1-3)	3 (2-4)	[11]
PECVD SiN - Upgrade to two sided processing	3200 (3040-3360)	wafer/h	6 (4-8)	1 (0.5-1.5)	3 (2-4)	[11]
Rear AlOx passivation Tool	3200 (3040-3360)	wafer/h	6 (4-8)	3 (2-4)	3 (2-4)	[11]
PERC Laser	3200 (3040-3360)	wafer/h	5 (3-10)	3 (2-4)	2 (1-3)	[11]
Screen Printer (Additional front print	3200 (3040-3360)	wafer/h	12 (6-14)	1 (0.5-1.5)	0 (0-0)	[11]
Screen Printer (2 prints)	3200 (3040-3360)	wafer/h	12 (6-14)	2 (1-3)	2 (1-3)	[11]
Dopant Spray Coater	3000 (2400-3600)	wafer/h	3 (2-5)	1 (0.5-2)	2 (1-3)	[12]
Doping Laser	1200 (960-1440)	wafer/h	5 (3-8)	1.5 (1-2)	2 (1-3)	[12]
Plating Tool	2400 (1920-2880)	wafer/h	4 (2-6)	1 (0.5-2)	2 (1-3)	[12]
Sinter Furnace	2400 (1920-2880)	wafer/h	3 (2-4)	0.5 (0.25-1)	2 (1-3)	[12]
Hydrogenation Laser	3600 (3240-3960)	wafer/h	5 (3-10)	0.5 (0.25-1)	2 (1-3)	[13]
LED Hydrogenation	3600 (3240-3960)	wafer/h	5 (3-10)	0.5 (0.25-1)	2 (1-3)	[13]
Hydrogenation Firing Furnace Upgrade	3200 (2880-3520)	wafer/h	3 (2-4)	0 (0-0)	1 (0-2)	[13]
Firing Furnace	3200 (3040-3360)	wafer/h	3 (2-4)	1 (0.5-1.5)	2 (1-3)	[11]
Cell test, sort and package	3200 (3040-3360)	wafer/h	5 (3-7)	3.5 (2.5-4.5)	2 (1-3)	[11]

For sequences A (Al-BSF) and B (PERC), data was taken from the 2017 ITRPV report [1]. Specifically, for p-type mono wafers, it predicts a 20% cell efficiency for Al-BSF and 21.2% cell efficiency for PERC processing in 2017.

Table S6 Material Cost Input Assumptions with Uncertainty Ranges - the usage assumptions are extrapolated from the data sources and estimated wastage rates for each process. Cost information taken from the data sources is adjusted to account for the passage of time and purchase volumes.

Process	Material	Unit	Usage (Unit/m^2)	Cost (US$/unit)	Ref
Wafer Cost	p-type wafer	wafer	1 (1-1)	0.798 (0.778-0.813)	[9]
Texture and damage etch	Texture Etch chemicals	per wafer	1 (1-1)	0.019 (0.013-0.024)	[11]
Emitter Diffusion	Diffusion chemicals	per wafer	1 (1-1)	0.053 (0.037-0.069)	[11]
PSG Removal and Edge Isolation	Rear Etch chemicals	per wafer	1 (1-1)	0.036 (0.025-0.046)	[11]
PECVD of SiNx:H (Front Only)	PECVD chemicals	per wafer	1 (1-1)	0.02 (0.014-0.026)	[11]
PECVD of SiNx:H (Rear Only)	PECVD chemicals	per wafer	1 (1-1)	0.02 (0.014-0.026)	[11]
Rear passivation AlOx	Rear SiN/AlOx gases	per Wafer	1 (1-1)	0.005 (0.004-0.007)	[11]
Screen Print 2 rear layers	Rear Pastes	per wafer	1 (1-1)	0.046 (0.032-0.06)	[11]
Screen Print 2 rear layers	Screen Print Screens	per 1k wafer	0.001 (0.001-0.001)	1.03 (0.719-1.34)	[11]
Screen Print front Ag	Front Ag paste	per wafer	1 (1-1)	0.046 (0.032-0.06)	[11]
Phosphorous spray coat	Phosphoric Acid	mL	0.4 (0.32-0.48)	0.005 (0.003-0.008)	[12]
Ni/Cu/Ag Plating	Ag plating Solution	per wafer	1 (1-1)	0.031 (0.015-0.046)	[12]
Ni/Cu/Ag Plating	Cu plating solution	per wafer	1 (1-1)	0.004 (0.002-0.005)	[12]
Ni/Cu/Ag Plating	Ni plating solution	per wafer	1 (1-1)	0.008 (0.004-0.011)	[12]

For sequence C (LDSE), since this process is not in commercial production, it is more difficult to estimate the performance of this sequence. In early production the Pluto process at Suntech was better than the standard Al-BSF sequence (2 months of production data), with a 5 %rel increase in current, a 2 %rel increase in voltage and 3 %rel increase in FF to achieve overall a 11 %rel (1.8 $\%_{abs}$) increase in efficiency [2]. However with current production cell efficiencies of Al-BSF close to 20 $\%_{abs}$ compared to the 16.5 % baseline at the time, the room for improvement is much reduced. We estimate that an improvement of 1 %rel in voltage and 1.5 %rel in current with an unchanged fill factor is possible in production, which would result in an overall cell efficiency boost of around 0.5 $\%_{abs}$. As there is some uncertainty in this, in the model we have assumed a cell efficiency boost of 0.4 $\%_{abs}$, and uncertainty range of $\pm$ 0.1 $\%_{abs}$.

For Sequence D (PERC + LDSE), we have estimated that compared to the PERC Sequence B, we would have a 0.9 $\%_{abs}$ increase in cell efficiency. This is based firstly on expected higher voltages. In development work of PERC + LDSE on p-type mono wafers [3], batch average voltages of 696 mV were obtained. This was for a modified industrial LDSE process (Suntech Power Pluto) on the front surface and a PERC structure on the rear that is expected to give similar performance to the current standard PERC process used in industry. In that work, a side by side comparison between PERC only and PERC + LDSE was not carried out, making a direct comparison difficult. However in 2016 Sunrise verbally reported an average voltage for PERC production cells of 670 mV[14]. We thus expect that in commercial production, the Voc can be enhanced by 3.7 %rel by adding the LDSE process to a PERC cell. The current would also be improved, because LDSE contact lines are thinner at 30 μm compared to standard screen print lines at 45 μm. We estimate that a 1 % increase in Isc is reasonable, and that fill factor should be unchanged by the LDSE process. These improvements can be calculated to contribute a 0.9 $\%_{abs}$ to the cell efficiency. In our model we use an uncertainty of -0.2 + 0.1 $\%_{abs}$.

For Sequences E (PERC + Laser H), F (PERC + LED H) and G (PERC + Furnace H), these each implement the UNSW advanced hydrogenation in different ways, however we expect that the hydrogenation performance would be equivalent to each other, though this would need to be checked with extended production testing. Some performance improvements for the Hydrogenation process have been reported by Hallam et al., where tests on CZ PERC cells showed that hydrogenation delivered both an as-produced efficiency gain as well as reducing the CID degradation. These two factors combined averaged 1.1 $\%_{abs}$. For one manufacturer, the data was presented showing that the as-produced

efficiency gain was $0.2\,\%_{\text{abs}}$ and the avoided degradation was $0.8\,\%_{\text{abs}}$ [5]. For the purposes of cell and module cost, we have only included the as-produced efficiency improvement, and have set this at $0.2 \pm 0.1\ \%_{\text{abs}}$. This efficiency improvement is varied for each sequence independently to allow any impact of performance differences between these processes to be understood.

The CID effect is analysed for its market effect as explained in Section S2.5.

S2.3 Module Manufacturing Costs and Module Performance

Cells must be assembled into modules, which includes serial and parallel electrical interconnection and encapsulation. There is significant research into alternative methods of module formation that can save cost or increase the power of the modules. As our focus in this study is the cell fabrication steps, but since we also need to consider the market price of completed modules, it is necessary to estimate the module manufacturing costs. Because there is scope for significant change in this area, we have modelled the total module manufacturing cost (including materials, equipment depreciation and running costs, labour and materials) as a single uncertain variable $CTMCost_i$.

This number was extracted from the Woodhouse et al. study [11], where module manufacture is estimated at 0.13$/w for a 310W module (i.e. $40.30/module), to which we have applied an uncertainty range of ±10%. This is consistent with the ITRPV report [1], which estimates that cell to module fabrication contributes 37% of the total cost of US$0.37/W in Q1 2017, which can be calculated as $0.137/W.

The moduling process also has an impact on the performance of the solar cells. Generally there is a loss of power from effects such as the additional reflection from the front glass, and shading from the interconnection [15]. For the purpose of this study, we have modelled this effect as a variable $CTMPower_i$, a ratio that also varies with uncertainty. We have used the same definition as the ITRPV [1] - "the total power output of the module divided by the total power output of the cells". The ITRPV report estimates the 2017 CTM ratio for mono c-Si modules at 98.5%. We have assumed this value with an uncertainty of $\pm 0.5\ \%_{\text{abs}}$. The reason for this variation is that this CTM factor can change depending on the module techniques used. For example, adding an anti-reflection coating on the front glass will increase this factor as well as increasing the cost. As our focus is on cell fabrication differences, we have assumed that this factor is identical for each production sequence.

Note that since we are modelling $CTMPower_i$ as the same for each Sequence, this neglects the possible effect of different spectral responses of each Sequence compared to each other. In particular, a selective emitter sequence would be expected to have an improved blue response, but blue light is often more strongly absorbed by the front glass. Thus a selective emitter cell would likely have a lower CTMPower parameter than a standard (homo) emitter cell. In our study we have assumed that such an effect is within the noise of the efficiency boost between Sequences (Table 1). The assumed range values for *CTMPower* are shown in Table 2.

S2.4 Module Price including Power Premium Calculations

To estimate $BaselineSellingPrice_i$ for a 280W module, we have taken 6 months of historical average spot prices for mono c-Si modules from April to Sept 2017 from EnergyTrend [9]. The average ($0.381/W), low ($0.375/W) and high ($0.385/W) values of this data were used as the Nom, Low and Hi values for this parameter.

We expect that a selling price premium can be obtained for higher module efficiency, since higher efficiency modules allows a more cost effective installed system cost (in $/W) where area related costs (such as land and mounting hardware) are significant. We also see this in practice, where for example mono c-Si modules consistently sell for higher prices (in $/W terms) than multi c-Si modules. It is difficult to calculate and justify a specific price premium on the basis of installed system cost, as this

is highly dependent on the specifics of each installation. However we have calculated the weekly price difference between mono and multi c-Si modules over a 6 month period [9] in c/W per Watt of additional module power (average 0.09, min 0.08, high 0.11). These ranges are used to generate the $PowerPremium_i$ parameters.

S2.5 CID Free Premium Calculations

The CID degradation effect has been shown to be 4%rel in some tests with commercially produced cells [5]. This degradation effect occurs gradually in the field, and then recovers. The exact timescale of both developing and recovering this effect depends strongly on the installation conditions. For example Lee et al. [16] suggests that leaving modules at open circuit in the field can recover CID within a period of one week, whilst modules installed "in operation" did not recover after a period of one month (although the modules were showing signs of slow recovery). Hallam et al. [17] have shown by modelling that it is possible to accelerate the degradation and recovery so that full recovery occurs after a period of a few weeks to a few years if the modules are left in the field at open circuit, and depending on the location and season of installation. However this requires the modules to be kept at open circuit while in the field, and is not practical to implement.

This uncertainty in the degradation makes it even more difficult to estimate the price premium a module supplier could expect from having a "CID Free" module. The size of this price difference will have a significant impact on the benefit to the manufacturer of this process. There are a number of ways to estimate the market impact of a CID-free module.

1) A branding effect that is not directly related to any specific metric. In other words, by saying that a module is CID free (and being able to back this up with test results), this increases the value of the brand by being judged as higher quality. The customer then will be willing to pay a price premium. This price premium may change over time as attitudes to CID change. E.g. if CID is seen by the market as a huge problem, this premium will be high. If it is seen as a minor inconvenience, then this premium may be low or non-existent. This effect may also be tempered by other brand related issues, such as the size and reputation of the manufacturing company.

2) De-rating module power by manufacturers. If manufacturers are concerned that their modules are not seen to be defective, they may choose to de-rate their module name plate power to account for CID effects. For example, module warranty conditions may allow for say 2.5% power drop within the first year, followed by a 0.7% drop each year subsequently (an example of such a warranty can be found in [18]). If any manufacturer is concerned that CID effects threatens to cause module returns, it may choose to de-rate the modules by say half the expected CID amount (2%rel). Another common metric used by end users is the "Performance Ratio", which is the number of kWh/year generated by a PV system compared to the amount expected if the modules maintained their rated power output. Derating modules that are CID affected would ensure that the modules maintained a high Performance Ratio. Any such derating to ensure high performance ratio or to ensure that the modules stay within the warranty power output conditions would result in a lower selling price and therefore margin to the manufacturers.

3) Customers willing to pay higher prices for CID-Free modules based on the expected generated electricity increase of their PV systems. This is a decision or analysis done by the module customers. If they are faced with a decision of whether to purchase "CID Free" modules or "Standard" modules, they may wish to calculate the expected effect on their system performance and how this impacts their financial performance. In that case, they need to estimate the total power loss during the life of the module. One way to assess this is in calculating the impact on LCOE. The LCOE calculates the total costs of the system over its lifetime, and divides this over the energy output over its lifetime to calculate the cost per unit energy (e.g. $/kWh) over its lifetime. There are many complications

to this calculation, such as the use of discount rates on the value of money, etc. For a very simple "back of the envelope" analysis we can say that if a module is expected by the customer to provide say 3% lower power output over the lifetime of the system compared to a CID-Free module, then the customer would calculate that the total output energy of the system is reduced by 3%. As PV system costs are dominated by up front capital costs, and as the PV modules make up approximately half of the total system cost, then the customer might consider a discount of 6% on CID-affected modules to be LCOE cost neutral. Note that this analysis depends strongly on the expectation of the customer of the change in power output. In the paper we also discuss the possible effect on "Bankability" of modules subject to degradation.

These three factors will impact the market price of such CID-Free modules, but the exact value to the market is not clear, and may also change over time as the understanding and attitude of manufacturers and end users changes. We have included a "CIDFreePricePremium" to Sequences E, F and G within our model, applying an uncertainty range within our Monte Carlo analysis. The nominal value in the model is 1 %rel with a low value of 0.5 %rel and a high value of 2 %rel as shown in Table 2.

S3 Cost Model Details

S3.1 Calculation of Process costs using Monte Carlo analysis

In the paper, a high level formula for Process Cost is provided (Equation 1). To explain in detail how this is derived, we have included a spreadsheet as additional supplementary material, which shows how the model generates the parameter values for each iteration, and then combines them to calculate the various cost components, and calculates the Normalised Uncertainty.

One important simplification in this model is that each production tool is assumed able to run at full capacity (less maintenance time) when calculating the depreciation and running costs. This neglects the normal factory requirement to tune the throughput of tools to closely match each other in multiple parallel lines. Because of the random nature of the Monte Carlo analysis, if this complication were to be included, it would result in wide variations in tool utilisation rates which would add variation to the results. By making this simplification, we are effectively assuming that for each iteration, a tool's cost per unit of production is fixed, but the actual cost and throughput of each tool can be optimised to match the rest of the factory. This simplification has some reflection in reality, where even though processes and technologies change over time, tool manufacturers will tend to design and offer production tools to match multiples of common industry standard throughput values, such as 3600 wafer/h.

The formula for generating iterations using the Log-Normal distribution are shown in Chang et al. [19], duplicated here in Equations 1, 2 and 3.

$$\sigma_H = \ln(Y_{High}/Y_{Nom})/1.28 \tag{1}$$

$$\sigma_L = \ln(Y_{Nom}/Y_{Low})/1.28 \tag{2}$$

$$Y_i = \begin{cases} Y_{Nom} \cdot \exp(\sigma_H \cdot Z_i) & \text{if } Z_i > 0 \\ Y_{Nom} \cdot \exp(\sigma_L \cdot Z_i) & \text{if } Z_i < 0 \end{cases} \tag{3}$$

This distribution does not always result in smooth distribution curves, with the possibility of discontinuities at the nominal value, as for example shown in Figure S1. This is because of the use of a two-half style distribution, where the two halves may not match at the median value. This can cause some lines in the scatterplots observed in Figure 5.

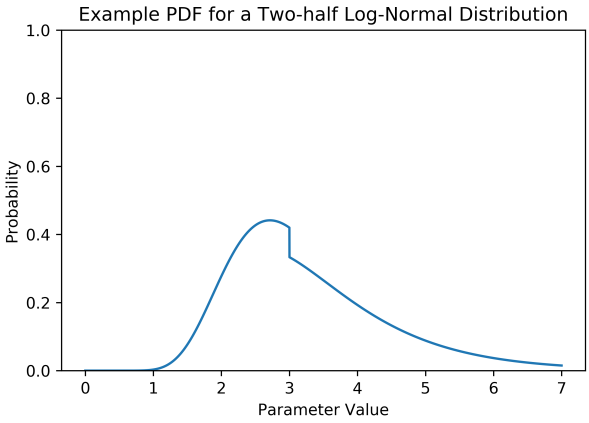

Figure S1 Example two-half log normal probability distribution with Low = 2, Nom = 3 and High = 5

S3.2 Impact of the number of Monte Carlo Iterations

Figure S2 shows the impact of changing i. Equivalent distributions to Figure 4a of the paper are shown with increasing i. As i increases, the smoothness of the distributions improves, but at the same time the computation time increases. At i=500, there is noticeable noise in the distribution graph (Figure S2a), which results in some variation in the extracted parameters if the simulation is run multiple times (Figure S2b). The noise in the distribution graph and the variation in the extracted parameters reduces significantly as i increases. i must thus be chosen to ensure that the variation of the extracted values should be much lower than the uncertainty we are attempting to measure with the Monte Carlo analysis. As discussed in the paper, $i = 5000$ was used to compute the model during data collection, since the simulation was run many times a day. $i = 50000$ was used once the data was finalised and to prepare metrics and figures for this paper.

S3.3 Modelling yield

Yield was been assumed at 100% in previous work [20]. Yield is a complex topic, as it comprises of a number of components. One factor, such as mechanical yield, is easy to measure in a running factory. However electrical yield is related to the cut-off of acceptable efficiency for a production line, and aesthetic yield may be based on a number of different criteria. Either of these requirements can change over time, changing the yield value even if there is no change in the production distribution.

In this work, we have included the average production cell fabrication yield as a randomly generated variable for each sequence. The purpose of this is to understand the relative sensitivity of the cost estimates to this factor, rather than as a prediction of factory yield based on experimental data.

It is not possible to use the two half log-normal distribution directly (Equations 1, 2 and 3) to generate $Yield_{Seq,i}$ from the Nominal, Low and High values given in Table 1, because this would generate yield values greater than 100%. To deal with this issue, we first transform each yield range parameter (e.g. $Yield_{Seq,Nom}$) into an equivalent Mean Time Between Failure (MTBF) parameter in units of production (Equation 4). We then generate i values of MTBF ($MTBF_{Seq,i}$) using a two half Log Normal distribution. An example distribution of the generated MTBF values is shown in Figure S3a. Each of the i generated MTBF values is then transformed back into a percentage yield value (Equation 5), to give the i Yield values used in the cost calculations. An example distribution of the generated $Yield_{Seq,i}$ is shown in Figure S3b.

$$MTBF_{Seq,Nom} = \frac{100}{100 - Yield_{Seq,Nom}} \tag{4}$$

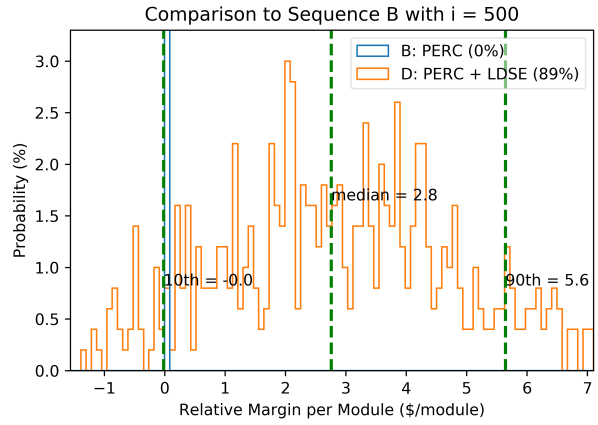

(a)

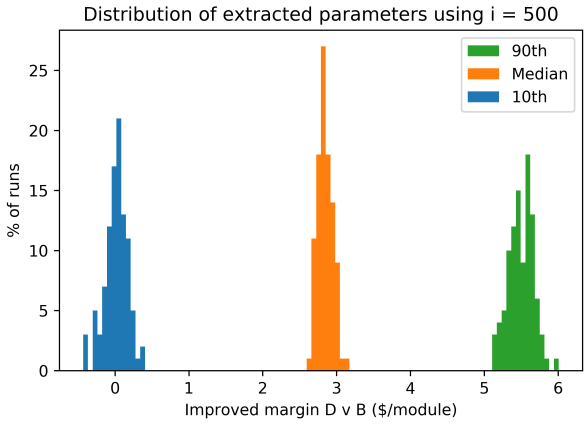

(b)

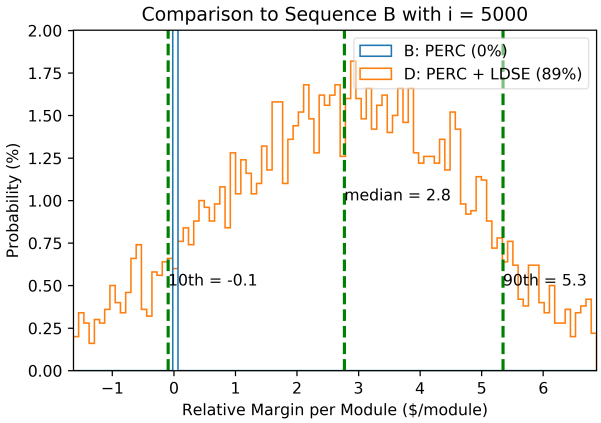

(c)

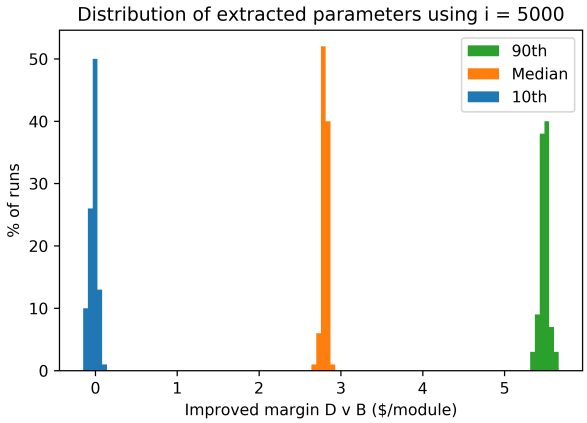

(d)

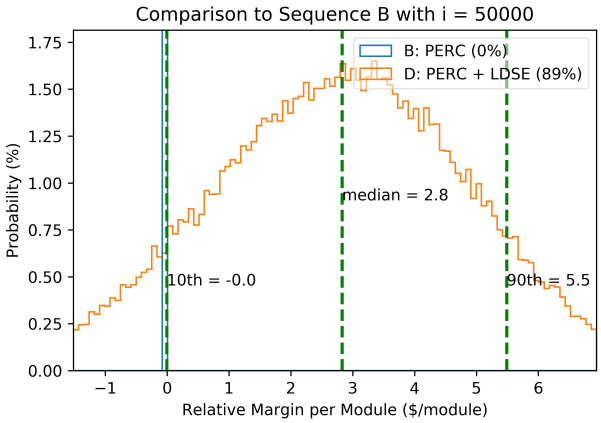

(e)

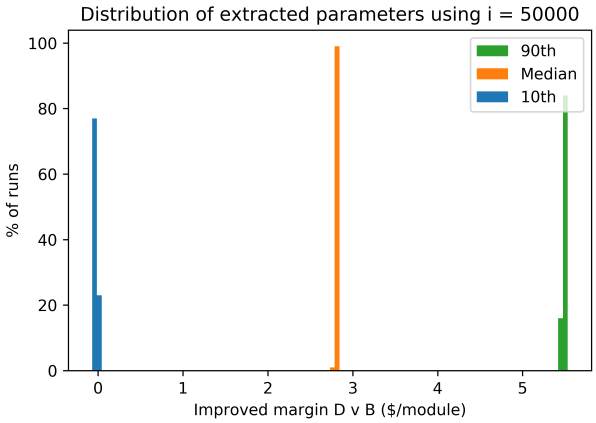

(f)

Figure S2 Impact of the selection of the number of iterations (i) on the Monte Carlo analysis. (a), (c) and (e) show example distributions similar to Figure 4a, but with varying i. (b), (d) and (f) show the distribution of extracted parameters from running the Monte Carlo Simulation 100 times for each selection of i. Note that these runs were completed independently of the final run and graphs shown in the paper, and so (e) does not match exactly with Figure 4a.

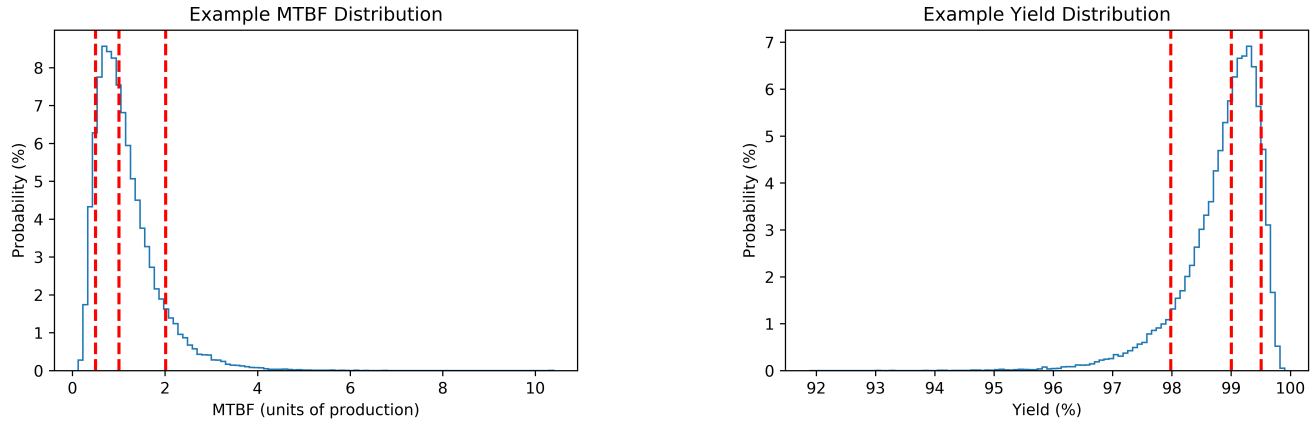

(a) **(b)**

Figure S3 Example generated distributions of a) Average factory MTBF and b) Average factory yield

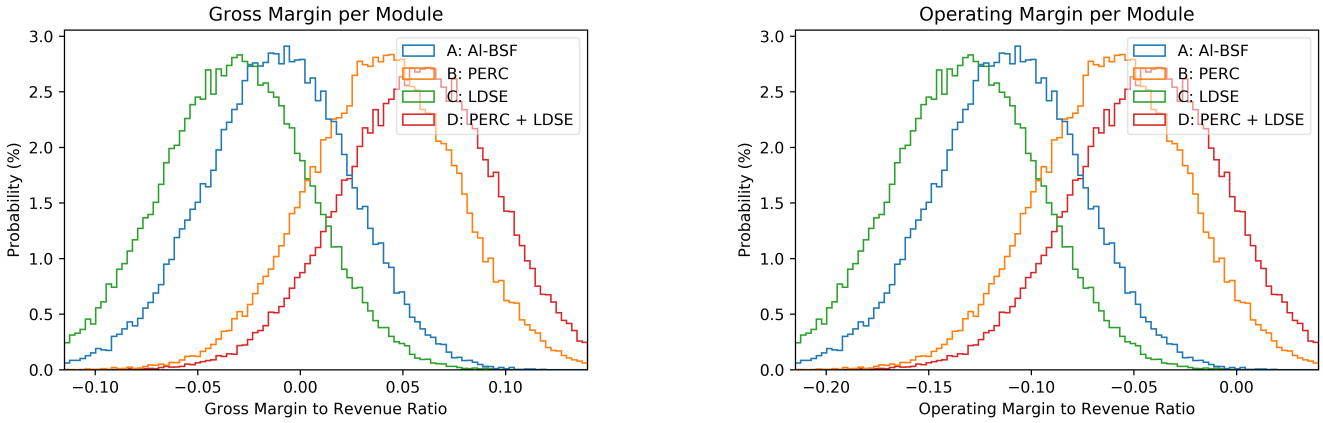

(a) **(b)**

Figure S4 Distribution of a) Gross Margin and b) Operating Margin for Seq A-D, as a ratio of revenue. For the Operating Margin calculations, a fixed overhead assumption of 10% is used

$$Yield_{Seq,i} = 100 - \frac{100}{MTBF_{Seq,i}} \tag{5}$$

S3.4 Margin Calculations

In the paper we focus on gross margin, which is the selling price less manufacturing costs. An alternative metric is the operating margin, which includes overhead costs such as R&D, sales and administration costs. We have not modelled these overheads in detail, but can calculate the operating margin by applying an assumed overhead of 10% of revenue. In Figure S4 we show the distribution of the gross margin and the operating margin (both expressed as a ratio to revenue). These distributions have a similar range to that of recently reported industry margins as described in a SunShot report [21].

Table S7 Key parameters whose uncertainty causes the most variance in the margin per module of Sequence D

Parameter	Unit	Uncertainty Range	Variance (%)
CTM Cost	$/module	36.02 - 43.97	37
Cell Efficiency	$\%_{abs}$	21.8 - 22.34	19
Power Premium	c/W / module W	0.08 - 0.13	17
Baseline Module Price	$/W	0.37 - 0.38	6
CTM Ratio		0.97 - 0.98	4
p-type wafer (122)	$\$/m^2$	28.5 - 29.8	3
Ag plating Solution (110)	$\$/m^2$	0.57 - 1.7	2
All other			12

S4 Additional Results

S4.1 Al-BSF, PERC and LDSE

In the paper, we show the contribution to variation of the various input parameters on the *MarginDiff* parameter. It is also possible to conduct the Contribution to Variance analysis on each Sequence separately. For example here in in Table S7 is the contribution to variance table for $Margin_{SeqD}$. We see here that the uncertainty in the cost of the upstream and downstream steps in the value chain are particularly important, as well as the Cell Efficiency and the expected Power Premium. Further work to reduce the uncertainty in those costs and parameters will reduce the distribution width of this sequence.

However in this work we are more interested in understanding the relative merits of one sequence compared to another, and the upstream and downstream processes are in this analysis common to each sequence. So by using the Simultaneous Monte Carlo analysis and applying the contribution to variance analysis on *MarginDiff*, as we have discussed in the paper, we can clearly see the parameters that most impact the commercial viability of implementing a process change.

S4.2 Additional Results - Advanced Hydrogenation

In Figure S5 we see the equivalent graphs to Figure 6, but showing the absolute difference instead of the percentages.

In the paper, Figure S5 compares three hydrogenation sequences (E, F and G) to PERC (Sequence B). This showed that each of the Hydrogenation sequences has a similar improved margin compared to the PERC baseline. In Table 5 the contribution to variance table on $MarginDiffCID_{SeqE,SeqB}$ was provided. Here, in figure S6, we show visually the impact of the four most significant variables.

In Figure S7 we additionally compare in more detail the three Advanced Hydrogenation sequences (E, F and G) with each other. First, we compare the margin of Sequences F and G compared to Sequence E (Figure S7a). This shows that within the uncertainties of this study, each Hydrogenation sequence is nearly indistinguishable from the other, with Sequence G (Furnace Hydrogenation) on average the best (by a very small amount) sequence. Using the Contribution to Variance analysis on the parameter $MarginDiffCID_{SeqG,SeqE}$, we see that the main causes of uncertainty in whether Furnace Hydrogenation is better than Laser Hydrogenation are the Efficiency Difference (71% of variation, Figure S7b) and the Yield difference (29% of variation, Figure S7c). All other factors contribute less than 1% to the variation. This shows us that the most important factor in choosing between Hydrogenation methods is the performance rather than the actual cost of the hydrogenation processes.

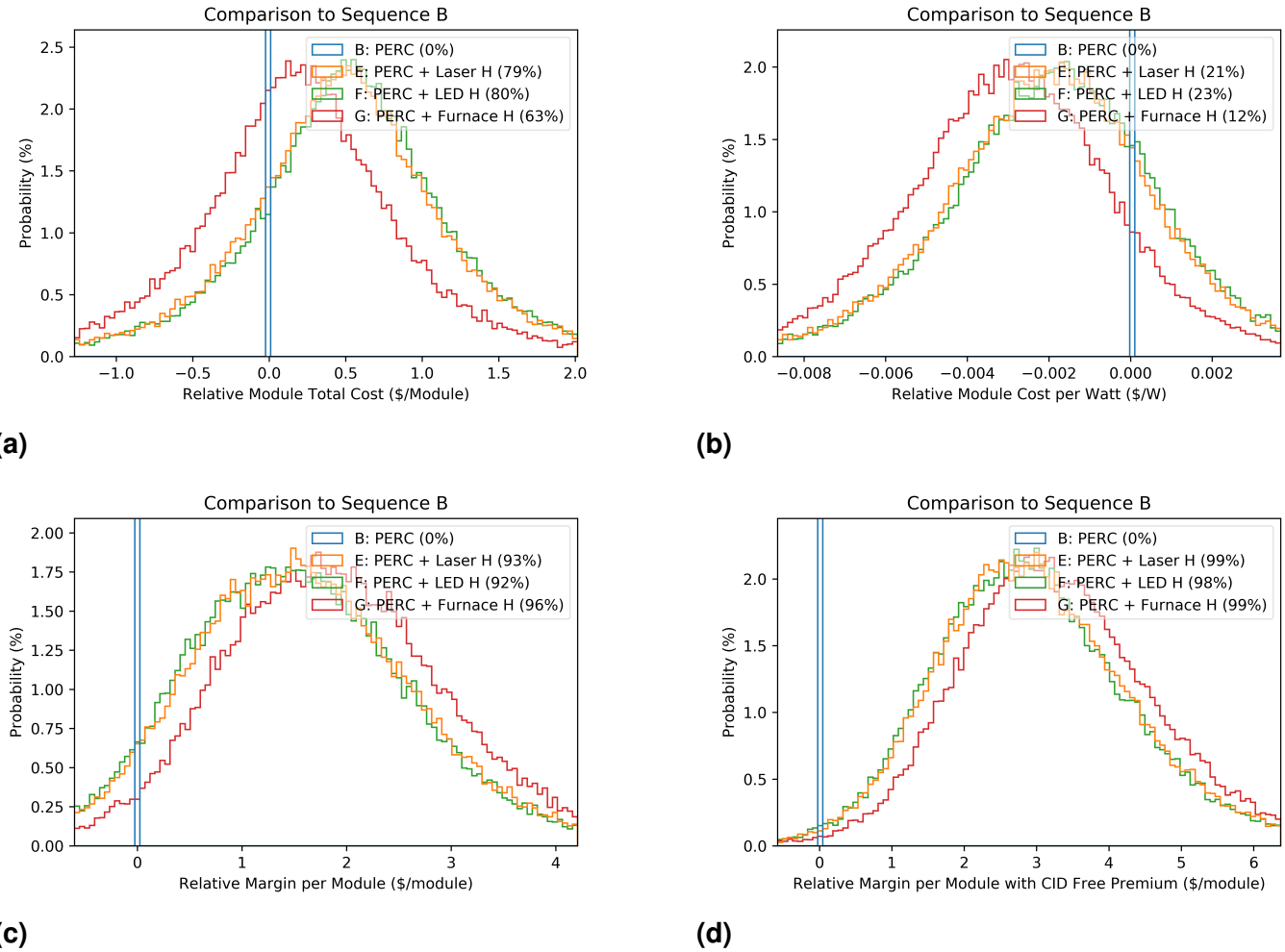

Figure S5 Cost distribution of the various Hydrogenation processes compared to the baseline PERC only sequence in a)US$/module b) module cost US$/W, c) margin per module in US$/module and d) margin per module in US$/module assuming a variable price premium for being CID Free

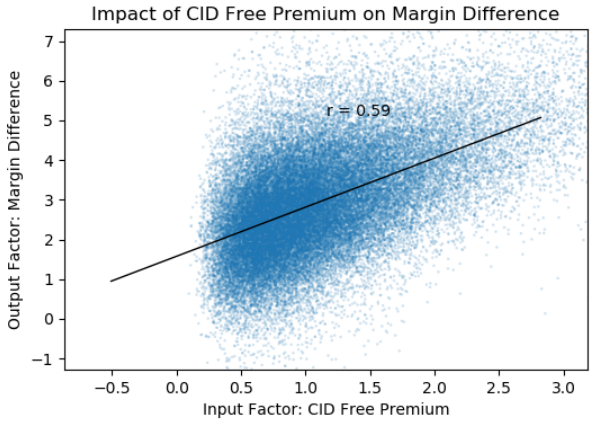

(a)

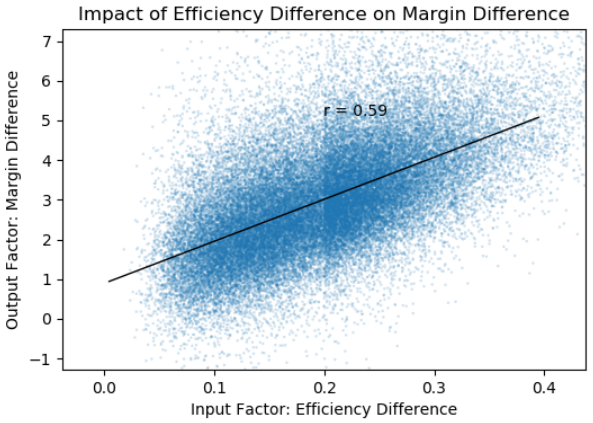

(b)

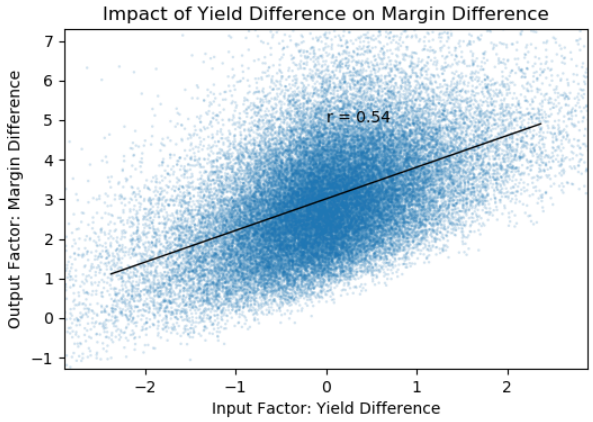

(c)

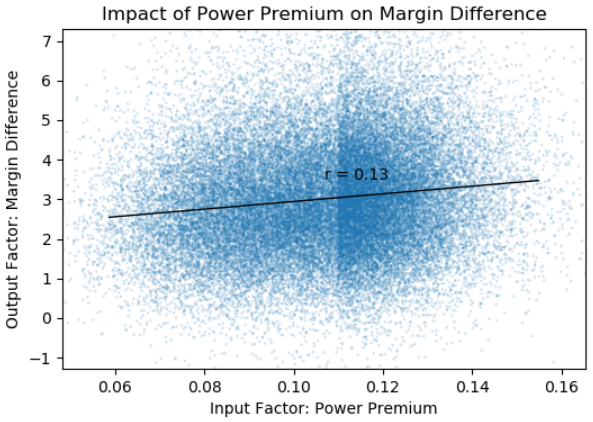

(d)

Figure S6 Scatter plots of key variables and their impact on the margin improvement of Sequence E compared to Sequence B, assuming a variable price premium for CID-Free modules

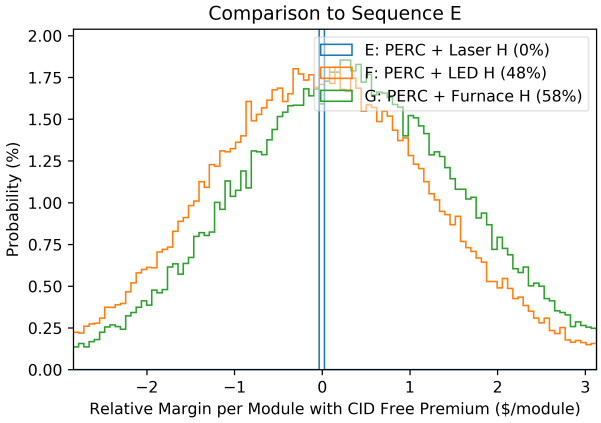

(a)

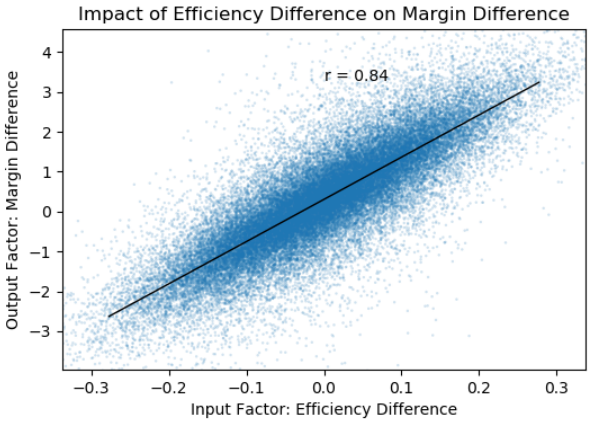

(b)

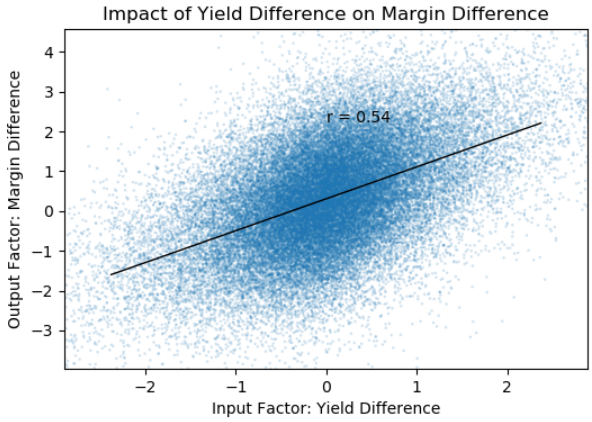

(c)

Figure S7 a) Compares Seq F and Seq G with Seq E as the baseline. b) and c) show the impact of the relative efficiency gain and relative yield on the $MarginDiff_{SeqG,SeqE}$

References

[1] ITRPV Eighth Edition 2017. http://www.itrpv.net/.cm4all/iproc.php/ITRPV%20Eighth%20Edition%202017.pdf?cdp=a. Accessed: 2017-05-01.

[2] Shi Z, Wenham S, Ji J. Mass production of the innovative PLUTO solar cell technology. *Photovoltaic Specialists Conference (PVSC), 2009 34th IEEE*. IEEE, **2009**; 001922–001926.

[3] Ciesla A, Chen R, Wang S, Ji J, Shi Z, Mai L, Chan C, Hallam B, Chong C, Wenham S, Green M. High-voltage p-type PERC solar cells with anchored plating and hydrogenation. *Progress in Photovoltaics: Research and Applications* ; .

[4] Wenham A, Chong CM, Wang S, Chen R, Ji J, Shi Z, Mai L, Sugianto A, Abbott M, Wenham S, et al. Copper plated contacts for large-scale manufacturing. *Photovoltaic Specialists Conference (PVSC), 2016 IEEE 43rd*. IEEE, **2016**; 2990–2993.

[5] Hallam B, Chan C, Payne D, Lausch D, Glaeser M, Abbott M, Wenham S. Techniques for mitigating light-induced degradation (LID) in commercial silicon solar cells. *Photovoltaics International* **2016**; **33**: 37–46.

[6] Hallam BJ, Chan CE, Chen R, Wang S, Ji J, Mai L, Abbott MD, Payne DNR, Kim M, Chen D, Chong C, Wenham SR. Rapid mitigation of carrier-induced degradation in commercial silicon solar cells. *Japanese Journal of Applied Physics* **2017**; **56(8S2)**: 08MB13.

[7] Goodrich AC, Powell DM, James TL, Woodhouse M, Buonassisi T. Assessing the drivers of regional trends in solar photovoltaic manufacturing. *Energy & Environmental Science* **2013**; **6(10)**: 2811–2821.

[8] Powell DM. c-Si PV Cost Model. https://pv.scripts.mit.edu/wp-content/uploads/2013/10/c-Si-Solar-Cost-Model_v2_0.xlsx. Accessed: 2016-06-03.

[9] EnergyTrend Website. http://pv.energytrend.com/pricequotes.html. Data from April 2017 until September 2017.

[10] Powell DM, Fu R, Horowitz K, Basore PA, Woodhouse M, Buonassisi T. The capital intensity of photovoltaics manufacturing: barrier to scale and opportunity for innovation. *Energy & Environmental Science* **2015**; **8(12)**: 3395–3408.

[11] Woodhouse M, Feldman D, Fu R, Ramdas A, Margolis R. Economic Factors of Production Affecting Current and Future Crystalline Silicon Photovoltaic Manufacturing Costs and Sustainable Pricing. *Paper Under Preparation, data taken from May 2017* ; .

[12] Edwards M. Efficiencies of 22% at low cost: the future of mass-produced laser-doped selective emitter solar cells. *Photovoltaics International* **2011**; **10**: 72–78.

[13] Personal Communication - Solar Industrial Research Facility, UNSW. Dates: 2016-Dec and 2017-Jun.

[14] Conference Presentation by Budi Tjahjono (Sunrise Global Solar Energy Co). PV Cell tech, Malaysia, Mar 2016.

[15] Haedrich I, Eitner U, Wiese M, Wirth H. Unified methodology for determining CTM ratios: Systematic prediction of module power. *Solar Energy Materials and Solar Cells* **2014**; **131**: 14–23.

[16] Lee K, Kim M, Lim JK, Ahn JH, Hwang MI, Cho EC. NATURAL RECOVERY FROM LID: REGENERATION UNDER FIELD CONDITIONS? *European Photovoltaic Solar Energy Conference (EUPVSEC), 31st*. EUPVSEC, **2015**; 1835–1837.

[17] Hallam B, Bilbao J, Payne D, Chan C, Kim M, Chen D, Gorman N, Abbott M, Wenham S. Modelling the Long-Term Behaviour of Boron-Oxygen Defect Passivation in the Field Using Typical Meteorological Year Data (TMY2). *European Photovoltaic Solar Energy Conference (EUPVSEC), 32nd*. EUPVSEC, **2016**; 555–559.

[18] Canadian Solar Standard Module Warranty. https://www.canadiansolar.com/downloads/warranties/en/Canadian_Solar-PV_Module_Warranty-en.pdf. Accessed: 2017-10-03.

[19] Chang NL, Ho-Baillie AWY, Vak D, Gao M, Green MA, Egan RJ. Manufacturing cost and market potential analysis of demonstrated roll-to-roll perovskite photovoltaic cell processes. *Solar Energy Materials and Solar Cells* **2018**; **174**: 314–324.

[20] Chang NL, Ho-Baillie AW, Basore PA, Young TL, Evans R, Egan RJ. A manufacturing cost estimation method with uncertainty analysis and its application to perovskite on glass photovoltaic modules. *Progress in Photovoltaics: Research and Applications* **2017**; **25(5)**: 390–405.

[21] Sunshot Q1/Q2 2017 Solar Industry Update. https://www.nrel.gov/docs/fy17osti/69107.pdf. Accessed: 2017-10-06.